BOREAS An international journal of Quaternary research

# The growth mechanism of the aragonitic stalagmite laminae from Yunnan Xianren Cave, SW China revealed by cave monitoring

WUHUI DUAN, BINGGUI CAI, MING TAN, HONG LIU AND YONG ZHANG

BOREAS

Duan, W., Cai, B., Tan, M., Liu, H. & Zhang, Y. 2012 (January): The growth mechanism of the aragonitic stalagmite laminae from Yunnan Xianren Cave, SW China revealed by cave monitoring. *Boreas*, Vol. 41, pp. 113–123. 10.1111/j.1502-3885.2011.00226.x. ISSN 0300-9483.

Stalagmites from Xianren Cave in Yunnan Province, SW China have visible bands of alternating compact and porous sub-layers, which have recently been demonstrated to be annual: the compact sub-layer consists of elongated columnar aragonites with a general longitudinal orientation (parallel to the vertical growth axis), while the porous sub-layer is composed mainly of needle aragonites forming radiating masses. In order to understand the growth mechanism of this type of stalagmite laminae, factors that could determine the growth rate and crystal structures of modern carbonates, such as cave-air temperature, $CO_2$ concentration, drip rate and the hydrochemical parameters of drip water, have been monitored systematically. In this study, we selected five active drip sites to monitor for two years at a monthly frequency. Based on the monitoring results and the analyses of stalagmite laminae, we conclude that the compact sub-layer forms in winter, when the drip rate is moderate and the degassing is slow, continuous and prolonged. The porous sub-layer forms in early spring, when the drip rate is lower and Mg/Ca is higher than that during the formation of the compact sub-layer. We also found exceptionally some calcite laminae. Furthermore, we discovered modern calcites precipitating at all study sites in the first hydrologic year when the rainfall was very abundant. Therefore, it is suggested that the occurrence of localized calcites in an aragonitic stalagmite indicates an interval of higher rainfall.

*Wuhui Duan (e-mail: duanwuhui@mail.iggcas.ac.cn) and Ming Tan (e-mail: tanming@mail.iggcas.ac.cn), Key Laboratory of Cenozoic Geology Environment, Institute of Geology and Geophysics, Chinese Academy of Science, Beijing 100029, China; Binggui Cai (e-mail: bingguicai@qq.com), National Research Center for Geoanalysis, Beijing 100037, China; Hong Liu (e-mail: hongliu@ynu.edu.cn), Yun Nan University, Kunming 650091, China; Yong Zhang (e-mail: zyongbj@126.com), National Gems & Jewelry Technology Administrative Center, Beijing 100013, China; received 7th March 2011, accepted 15th June 2011.*

So far, five main types of stalagmite laminae have been reported as follows: (i) fluorescent laminae formed by annual variations in organic matter flux (Baker *et al.* 1993; Tan *et al.* 1999; Proctor *et al.* 2000), (ii) visible or petrographic laminae formed by annual variations in calcite texture or fabric (Genty 1992; Tan *et al.* 1997; Polyak & Asmerom 2001; Soubies *et al.* 2005), (iii) calcite–aragonite couplets (Railsback *et al.* 1994; Denniston *et al.* 2000), (iv) trace-element laminae (Fairchild *et al.* 2007), and (v) aragonitic laminae formed by the alternation of thin brown and thicker clear aragonitic sub-layers (Brook *et al.* 1999; Bertaux *et al.* 2002; Yadava *et al.* 2004; Cai *et al.* 2010, 2011; Duan *et al.* 2010). Changes in thickness through successive laminae of stalagmites have been used to extract palaeoclimatic information (Genty & Quinif 1996; Brook *et al.* 1999; Proctor *et al.* 2000; Frisia *et al.* 2003; Tan & Liu 2003). In addition, some monitoring investigations have been performed to study the formation process of stalagmite laminae (Bar-Matthews *et al.* 1991; Railsback *et al.* 1994; Frisia *et al.* 2000, 2002; Self & Hill 2003; Ban *et al.* 2008; Mattey *et al.* 2008; Cai *et al.* 2011; Ruan & Hu 2010). However, modern carbonate microstructures are rarely investigated, and their relationships with stalagmite laminae are not yet clear.

In 2003, we collected stalagmite specimens from Xianren Cave in Yunnan Province, SW China. Each of them consists mainly of aragonites. All the stalagmites have the same visible bands, showing alternation of compact and porous sub-layers, which have been shown to be annual laminae by comparing lamina counts with U-Th dates (Fig. 1A) (Duan *et al.* 2010). Similar couplets have been described in various aragonitic stalagmite studies. Brook *et al.* (1999) attribute the darker layers to either dust (mainly clay) accumulation on the surface of the speleothems or to increased incorporation of humic acids. Bertaux *et al.* (2002) suggest that the brown layers result from the incorporation of dissolved organic matter (DOC) in the aragonite crystals. Yadava *et al* (2004) consider the dark layers as $CaCO_3$ precipitated with the trapped detrital particles. In summary, all of the aragonitic stalagmite laminae reported earlier are characterized by compositional changes, but the stalagmite laminae from Xianren Cave are characterized by changes in the aragonite crystal structures of sub-layers. A preliminary study of stalagmite laminae showed that the compact sub-layer is composed of elongated columnar aragonites with a general longitudinal orientation (parallel to the vertical growth axis; Fig. 1B) so that inter-crystalline voids are few, which makes the structure compact, whereas the narrow dark sub-layer is composed of needle aragonites forming radiating masses so that there are many inter-crystalline voids (Fig. 1C), which makes the structure porous (Duan *et al.* 2010). However, no monitoring work aimed at investigating the growth mechanism of this type of stalagmites has been reported.

DOI 10.1111/j.1502-3885.2011.00226.x

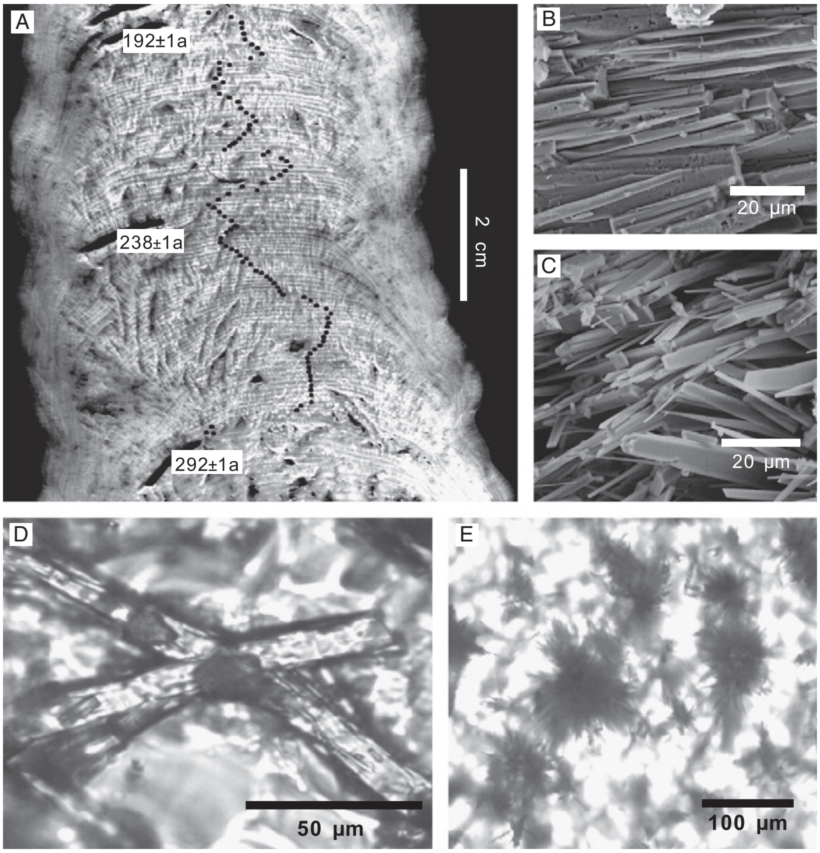

*Fig. 1.* Photographs of crystal structures of stalagmite laminae and modern aragonites precipitated on glass slides under the drip sites. A. Scanning image of stalagmite laminae showing alternating compact and porous sub-layers. The numbers are ages representing years before 2006. The dots are the layer-counting data. B. SEM micrograph of compact sub-layers. C. SEM micrograph of porous sub-layers. D. Micrograph of the modern carbonate precipitated on glass slides during winter in 2009. E. Micrograph of the modern carbonate precipitated on glass slides during spring in 2010. (A–C from Duan *et al.* 2010). This figure is available in colour at http://www.boreas.dk.

Moreover, we found exceptionally some calcite laminae (Fig. 2A); these are not very common and only a few have been reported (Denniston *et al.* 2000; Frisia *et al.* 2002). Hence, in order to extract true high-resolution climate signals from the stalagmite laminae, it is necessary to understand the relationship between crystal microstructures and the environment of their formation.

This study seeks to elucidate the growth mechanism of aragonitic stalagmite laminae by means of cave monitoring; in particular, it aims (i) to determine the mineral composition and crystal structures of modern carbonate precipitating on glass slides placed under active drip sites, and (ii) to investigate the effects of the related environmental parameters, such as cave air $CO_2$ concentration, cave air temperature and humidity, drip rate, drip-water geochemistry and the growth rate of modern carbonate.

## Geological and environmental setting

Xianren Cave (104°08′56″E, 24°07′43″N, 1443 m a.s.l.) is located in SW China, about 286 km from Kunming city (Fig. 3). It is found in a karst highland of SE Yunnan Province, within a tropical monsoon zone. The local present-day climate is warm and humid. More than 80% of the total annual precipitation falls in summer (June to August). The mean annual temperature and precipitation recorded by the local metrological station are 16.7 °C and 1143.2 mm, respectively (the data are available in the local weather bureau report ‘The Evaluation of Climatic Effect of Qiubei County in 2010’). During the two hydrologic years of monitoring, the temperature outside the cave showed obvious seasonal variety. From July to December, the monthly average temperature decreased gradually from about 24 °C to 12 °C, and then it increased gradually to 24 °C again in summer (Fig. 4). The rainy season is in summer and autumn. The precipitation in the first hydrologic year (from August 2008 to August 2009) was much higher than that in the second year (from August 2009 to August 2010) (Fig. 5).

The bedrock above the cave is the massive grey dolostone in the middle Triassic–lower Tuowei formation, with a 330° strike and 12° dip. The soil above the cave is brown, typically less than 40 cm thick, and found only in rock fissures. The overlying vegetation is mainly liana shrubs and is so sparse that some parts of the rock are bare.

The cave system comprises a main passage opened for tourists and a branch just for research work, the two being connected by an underground river. Along the research passageway, three stalagmite specimens were collected for study in 2003, and five drip sites under the active stalactites were selected for monitoring (Fig. 3).

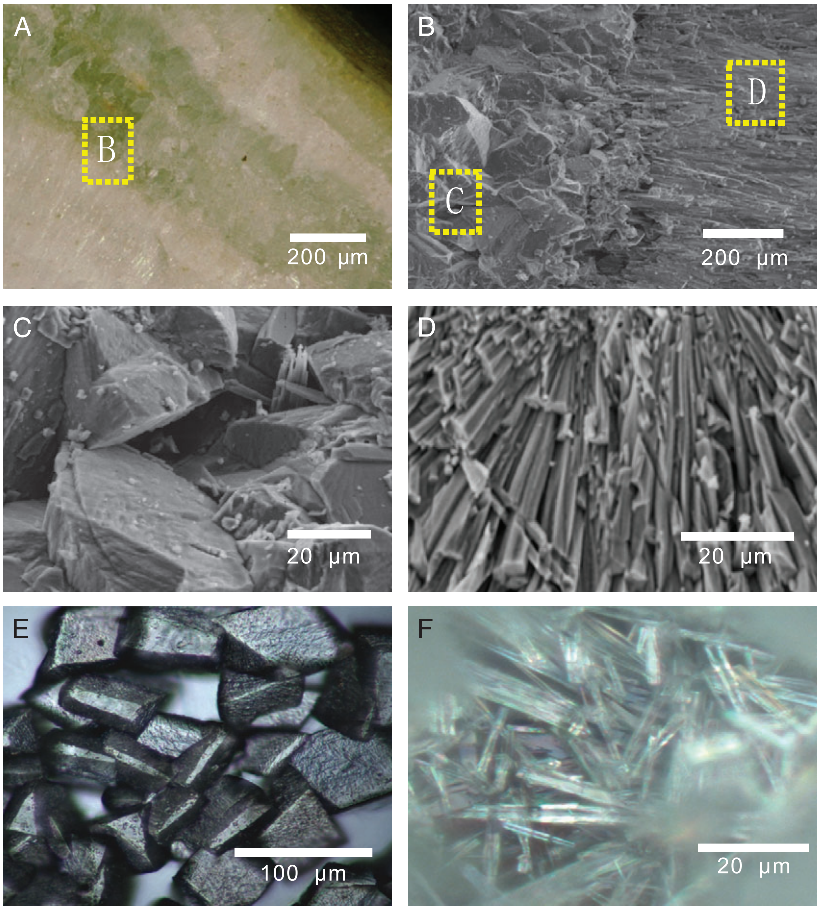

*Fig. 2.* Photographs of calcites and aragonites in stalagmite and modern carbonates precipitated on glass slides under the drip sites. A. Microphotograph of a stalagmite. B. SEM micrograph of the area identified in A. C. SEM micrograph of area C identified in B. D. SEM micrograph of area D identified in B. E. Micrograph of modern carbonate precipitated on glass slides in winter in 2008. F. Micrograph of modern carbonate precipitated on glass slides during spring in 2008. This figure is available in colour at http://www.boreas.dk.

## Methods

The temperature outside Xianren Cave was recorded automatically from August 2008 to August 2010 by a HOBO Temp/RH Data Logger (part number: H08-003-02; temperature range: −20 to 70°C, accuracy: ±0.7°C; humidity range: 25–95%, accuracy: ±5%). The logger was fixed in an instrument shelter near to the cave.

Precipitation in the Xianren Cave area has been measured automatically by a tipping-bucket rain gauge since September 2009 (Data Logging Rain Gauget-RG3-M; resolution: 0.2 mm). Before the rain gauge was fixed, rainfall data were obtained from the local weather station about 10 km from the cave.

Cave-air temperature and relative humidity were measured about every month using a handheld HANNA

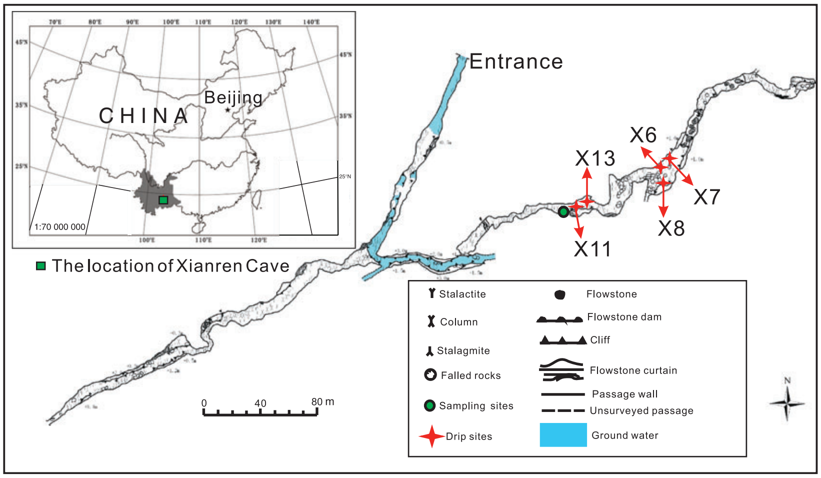

*Fig. 3.* Location of Xianren Cave and a plan view of its cave system. X6, X7, X8, X11 and X13 indicate the locations of drip sites. This figure is available in colour at http://www.boreas.dk.

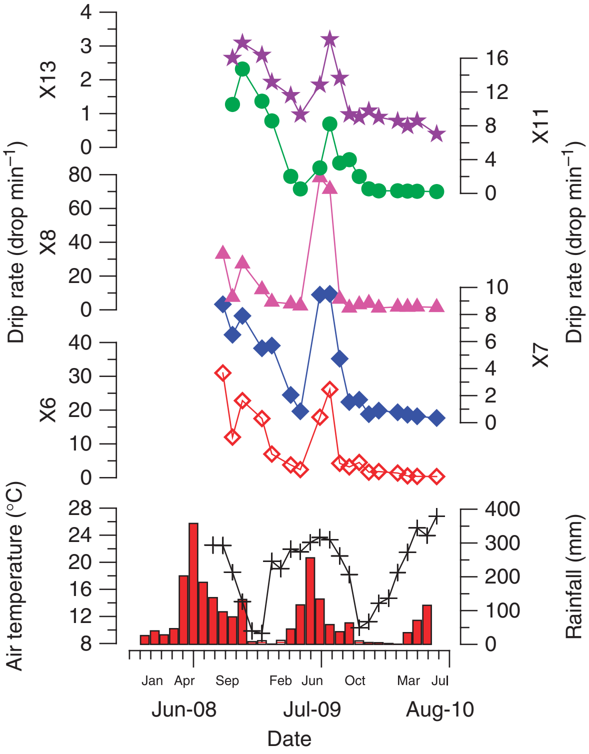

*Fig. 4*. Comparison of drip rate, monthly rainfall and temperature for the period between August 2008 and August 2010. X6, X7, X8, X11 and X13 indicate drip sites. This figure is available in colour at http://www.boreas.dk.

instruments HI 8564 thermo-hygrometer (resolution: RH: 0.1%; T: 0.1 °C). Cave-air $CO_2$ concentration was measured during each visit using a handheld Telaire 7001 meter (resolution: 1 ppm). $CO_2$ data are reported as concentration (ppmv).

For each study site (X6, X7, X8, X11 and X13), the drip water was collected in a 500-ml HDPE bottle that was fixed under the drip site for one night to collect enough water every time the cave was visited. Aliquots for cations were acidified in the field using super-pure nitric acid, stored in 30-ml HDPE sealed bottles, and taken to a laboratory for Na, K, Ca and Mg analysis. Drip rates were estimated by taking repeat counts of drops over 1 min or by determining the elapsed time between two drops and then taking the average; the relative error is less than 2%. Drip-water temperature and pH were measured with a HANNA HI8424 portable pH meter (resolution: 0.01), and electric conductivity (EC) was measured with a HANNA HI8733 portable EC meter (resolution: 0.01). Regarding alkalinity, because the pH was between 7.4 and 8.2, the $CO_3^{2-}$ concentration was so low that the alkalinity could be described approximately as $HCO_3^-$ concentration. It was determined by titration with 0.01 mol L$^{-1}$ hydrochloric acid *in situ*, using methyl orange as an indicator, yielding a measurement uncertainty of less than 0.1 mg L$^{-1}$. Cations were analysed using a Thermo IRIS ICP-OES (Thermo Elemental, Franklin, MA) with a ±10% accuracy range, and anions by liquid chromatography (Shimadzu, Mode LC-10AD), with an accuracy of ±5%. Saturation state (accuracy: ±0.1 units), which is defined as the logarithm of the quotient of the ionic activity product and solubility product, was calculated using the updated MIX 4 program (Fairchild *et al.* 2000). The drip-water supersaturation proxies (referred to as 'SI' hereafter) with respect to calcite and aragonite are reported as SIc and SIa, respectively, for convenience. At each drip site, a square glass slide (5×5×0.5 cm$^3$), which was sandblasted to simulate a stalagmite top, was placed horizontally and changed usually every month. The amount of carbonate growing during a given time interval was determined by weighing each dried glass slide before and after its deployment with a Sartorius BP211D electronic balance, yielding a standard deviation of 0.05 mg.Meanwhile, the mineral formed during the given time interval was observed under an optical microscope.

The laboratory analyses were undertaken at the Institute of Geology and Geophysics, Chinese Academy of Science.

## Results

Because the variation trend of the monitoring results of all five study sites are similar (Table 1), we show only two of them, X7 and X13, in this paper. At all the study sites, the cave-air temperature and relative humidity did not vary much during the whole year, with mean values of about 18.6 °C and 100%, respectively (Fig. 6). Seasonal variation of cave-air $CO_2$ concentration followed a sinusoidal

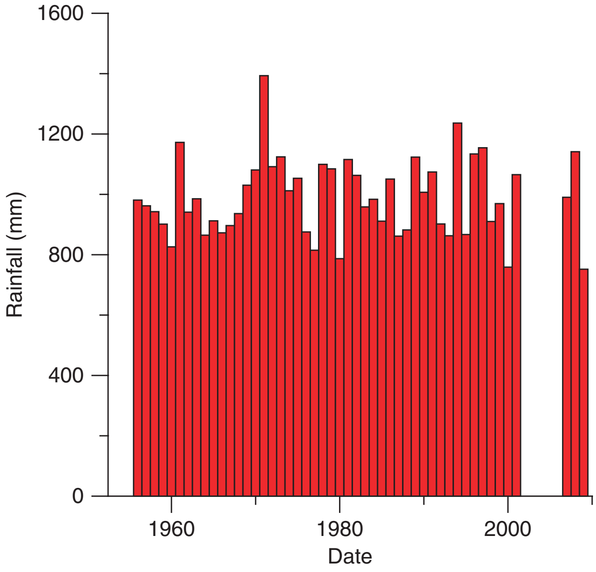

*Fig. 5*. Variations in local annual rainfall between 1954 and 2010. The data between 2002 and 2006 are missing. This figure is available in colour at http://www.boreas.dk.

*Table 1.* Seasonal averages of drip-site physical and chemical parameters.

| Drip site | Date | Growth rate (mg day$^{-1}$) | EC (μs cm$^{-1}$) | Drip rate (drop min$^{-1}$) | Water temp. (°C) | Cave-air $CO_2$ (ppmv) | Cave-air temp. (°C) | RH (%) | pH | $Ca^{2+}$ (mg L$^{-1}$) | $Mg^{2+}$ (mg L$^{-1}$) | $SO_4^{2+}$ (mg L$^{-1}$) | $HCO_3^-$ (mg L$^{-1}$) | SIc | SIa |
|---|---|---|---|---|---|---|---|---|---|---|---|---|---|---|---|
| X6 | Sep-08 to Apr-09 | 0.96 | 615 | 15.7 | 19.3 | 4910 | 18.7 | 100 | 7.76 | 69.2 | 49.5 | 3.2 | 447 | 0.47 | 0.26 |
| | May-09 to Aug-09 | 0 | 625 | 15.5 | 19.1 | 8967 | 18.7 | 100 | 7.45 | 69.2 | 44.0 | 4.2 | 507 | 0.27 | −0.02 |
| | Sep-09 to Apr-10 | 0 | 541 | 2.5 | 19.1 | 3162 | 18.7 | 100 | 7.91 | 35.2 | 50.7 | 4.5 | 381 | 0.34 | 0.11 |
| | May-10 to Jul-10 | 0 | 452 | 0.4 | 19.5 | 5935 | 18.7 | 100 | 7.49 | 47.8 | 62.0 | 3.5 | 351 | 0.09 | −0.12 |
| X7 | Sep-08 to Apr-09 | 0.41 | 576 | 6.1 | 19.3 | 4910 | 18.7 | 100 | 7.71 | 60.2 | 46.0 | 6.7 | 410 | 0.43 | 0.21 |
| | May-09 to Aug-09 | 0 | 692 | 6.7 | 18.9 | 8967 | 18.7 | 100 | 7.45 | 76.4 | .49.4 | 8.0 | 352 | 0.35 | 0.14 |
| | Sep-09 to Apr-10 | 0 | 614 | 1.5 | 18.5 | 3162 | 18.7 | 100 | 7.85 | 41.4 | 43.6 | 7.1 | 353 | 0.27 | 0.05 |
| | May-10 to Jul-10 | 0 | 476 | 0.4 | 20.4 | 5935 | 18.7 | 100 | 7.52 | 50.9 | 50.6 | 6.3 | 340 | 0.10 | −0.12 |
| X8 | Sep-08 to Apr-09 | 1.42 | 669 | 14.7 | 19.2 | 4910 | 18.7 | 100 | 7.72 | 65.6 | 52.8 | 3.7 | 484 | 0.41 | 0.19 |
| | May-09 to Aug-09 | 0.39 | 768 | 50.7 | 19.4 | 8967 | 18.7 | 100 | 7.40 | 87.9 | 52.8 | 4.8 | 411 | 0.43 | 0.21 |
| | Sep-09 to Apr-10 | 0.19 | 611 | 2.7 | 18.4 | 3162 | 18.7 | 100 | 7.97 | 48.1 | 52.0 | 4.6 | 438 | 0.57 | 0.35 |
| | May-10 to Jul-10 | 0 | n.d. | 1.7 | 20 | 5935 | 18.7 | 100 | 7.65 | 57.7 | 62.3 | 4.2 | 439 | 0.38 | 0.17 |
| X11 | Sep-08 to Apr-09 | 1.2 | 533 | 9.4 | 19.1 | 1426 | 18.7 | 100 | 8.01 | 31.4 | 57.1 | 1.9 | 365 | 0.21 | −0.01 |
| | May-09 to Aug-09 | 0 | 584 | 4.0 | 18.8 | 5504 | 18.7 | 100 | 7.59 | 40.1 | 56.3 | 2.4 | 451 | 0.25 | 0.03 |
| | Sep-09 to Apr-10 | 0 | 501 | 1.6 | 19.0 | 2353 | 18.7 | 100 | 8.24 | 18.9 | 50.0 | 2.7 | 327 | 0.11 | −0.01 |
| | May-10 to Jul-10 | 0 | 492 | 0.2 | 20.2 | 4898 | 18.7 | 100 | 7.71 | 21.4 | 69.3 | 2.1 | 341 | −0.12 | −0.33 |
| X13 | Sep-08 to Apr-09 | 1.22 | 628 | 2.4 | 19.1 | 1426 | 18.7 | 100 | 7.88 | 45.7 | 49.3 | 2.2 | 394 | 0.48 | 0.26 |
| | May-09 to Aug-09 | 0.32 | 670 | 2.0 | 18.4 | 5504 | 18.7 | 100 | 7.55 | 49.8 | 57.9 | 2.6 | 481 | 0.21 | 0.00 |
| | Sep-09 to Apr-10 | 0.64 | 631 | 1.0 | 19.0 | 2353 | 18.7 | 100 | 8.00 | 49.3 | 57.9 | 2.9 | 453 | 0.67 | 0.45 |
| | May-10 to Jul-10 | 0 | 607 | 0.6 | 19.9 | 4898 | 18.7 | 100 | 7.80 | 53.0 | 71.6 | 2.8 | 456 | 0.51 | 0.30 |

pattern similar to that of meteorological temperature and monthly accumulated rainfall, with the highest value (more than 10 000 ppmv) observed in the rainy season (late July) and the lowest value (less than 1000 ppmv) during the dry season (December) (Fig. 6).

Although the absolute value of the drip rate is very different in each study site, the seasonal variations for all sites follow the same pattern, namely similar to that of monthly accumulated rainfall (with about a one-month lag) (Fig. 4).

The geochemical parameters of drip water, which control the growth rate, mineral composition and crystal structures of modern carbonates, show seasonal and annual variations. For each drip site, except X13, in the two hydrologic years, the growth rate was high in winter and spring from November to April, with low EC, alkalinity, $Ca^{2+}$ and $Mg^{2+}$ concentrations, low cave-air $CO_2$ concentration and high pH and SI. In other months, however, the growth rate was near zero, and the cave-air $CO_2$ concentration and drip-water geochemical parameters showed opposite properties to those in winter and spring (Table 1; Fig. 7). One discrepant sampling period is at the end of the first winter at drip site X13. As shown in Fig. 7, the highest 'growth rate' occurs between two sampling

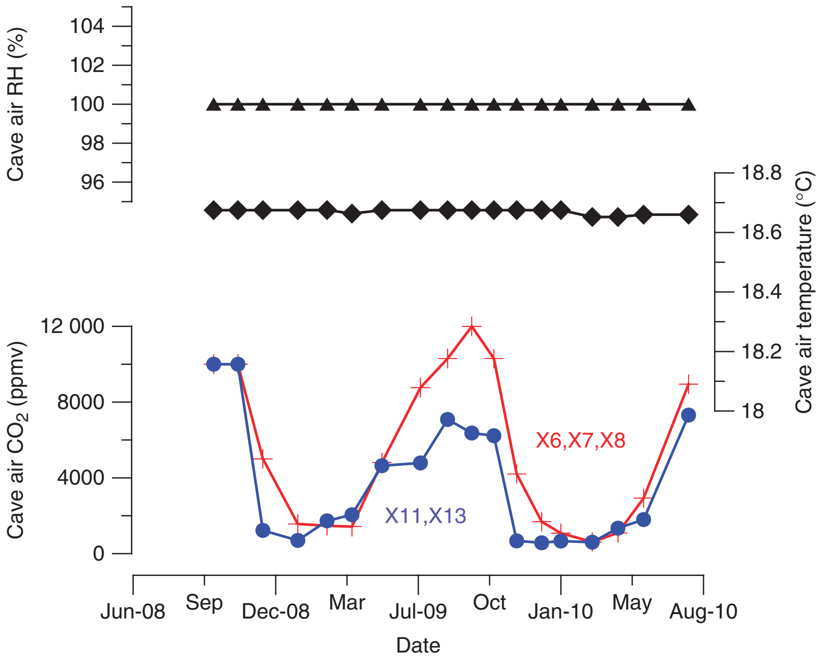

*Fig. 6*. Seasonal variations in cave-air $CO_2$ concentration, temperature and humidity for the period between August 2008 and August 2010. X6, X7, X8, X11 and X13 indicate drip sites. This figure is available in colour at http://www.boreas.dk.

intervals in which $Ca^{2+}$ and $Mg^{2+}$ concentrations are low and the calculated saturation index is negative. We used the spreadsheet that can predict EC from the ion analysis (Rossum 1975) to check the analytical problem about $Mg^{2+}$ and $Ca^{2+}$ concentrations. The results showed the predicted EC to be lower than what we measured immediately *in situ* in the cave, which means that the measured $Mg^{2+}$ and $Ca^{2+}$ concentrations may be lower than the real values. In turn, the calculated saturation index is negative at the end of the first year when the growth rate is highest. According to inter-annual variations, the growth rate in the first hydrologic year is much higher than that in the second, when the growth rate is non-zero only at sites X8 and X13. Furthermore, the rainfall and $Ca^{2+}$ concentrations of all the drip waters in the first hydrologic year are higher than those in the second (Table 1; Fig. 7), although for X13 the decreasing trend of $Ca^{2+}$ concentration is not very significant. However, there is an observable decreasing trend in the EC of X13 from the first year to the second.

The mineral composition and crystal structures of modern carbonates show visible variations. In the first hydrologic year, in winter from November to December, rhombohedral calcites formed on the glass slides with flat faces and few crystal defects (Fig. 2E) (Fig. 8). Subsequently, in late winter and early spring, from December to March (Fig. 8), needle aragonites gradually formed radiating masses (Fig. 2F). In the second hydrologic year, there were no calcities formed, but aragonites did, showing variable morphologies in different seasons. In winter, in about December (when the drip rate and SI are moderate) (Fig. 8), elongated columnar aragonites with flat faces and few crystal defects formed first (Fig. 1D). Subsequently, with the drip rate decreasing and Mg/Ca increasing (Fig. 8), much finer needle aragonites gradually formed radiating masses (Fig. 1E).

## Discussion

### *Factors controlling the growth rate of modern stalagmites in Xianren Cave*

Because the factors controlling the growth rate of stalagmites are so many and complex, we first use the supersaturation proxy (SI) to estimate the growth rate. $SI < 0$ means that equilibrium is not reached, and dissolution is possible. $SI > 0$ corresponds to an oversaturated solution in which only carbonate precipitation is possible. In general, more highly supersaturated solutions tend to precipitate $CaCO_3$ more quickly (Fairchild *et al.* 2007). The monitoring results of Xianren Cave are in agreement with the theory above: there is a strong positive correlation between the growth rate and SI value (Fig. 7). Regarding X13, we found some carbonate precipitated in the sample bottle at the end of the first winter, which could explain why when the growth rate is highest the SI value is negative. Because SI is calculated from many geochemical proxies of drip water and is also controlled by the kinetic factor-degassing (Holland *et al.* 1964), we will discuss each proxy below.

*pH.* – The higher pH and SI values coincide with the higher carbonate precipitation rates during the dry season (Fig. 7), which is in agreement with the study by Cai *et al.* (2011). This is because when pH is more than 8, the concentration of $CO_3^{2-}$ in drip water will increase with pH value, which will be beneficial to carbonate precipitation, whereas if pH is less than 8, the $CO_3^{2-}$ concentration will decrease, which will inhibit carbonate precipitation.

*Concentration of $HCO_3^-$.* – During summer the concentration of $HCO_3^-$ is high, and, as a result, the deposition rate is near zero, whereas during winter and spring the lower concentration of $HCO_3^-$ is coincident with a higher growth rate (Fig. 7). In other words, the correlation between the concentration of $HCO_3^-$ and carbonate growth rate is negative.

*Concentration of $Ca^{2+}$.* – $Ca^{2+}$ concentration of drip water has been reported to be positively correlated with stalagmite growth rate, and has been suggested to be a primary control on stalagmite growth in some cases (Baker & Genty 1998; Baker *et al.* 1998; Dreybrodt 1999; Genty *et al.* 2001). In our study, however, the measured $Ca^{2+}$ concentration of drip water is negatively correlated with the intra-annual carbonate growth rate, with the lowest growth rate coinciding with the highest $Ca^{2+}$ concentration during the summer monsoon rainy season, and the highest growth rate coinciding with lowest $Ca^{2+}$ concentration in the dry season (Fig. 7). The result is in agreement with the previous study in Shihua Cave, China (Cai *et al.* 2011). We conclude, therefore, that $Ca^{2+}$ is not a sufficient but is a necessary condition for carbonate growth. In other words, some other inhibitory factor may have a more intensive effect than $Ca^{2+}$ concentration. This will be discussed below.

The inter-annual carbonate growth rate is lower during the second hydrologic year than it is during the first, which coincides with the measured inter-annual variations in $Ca^{2+}$ concentration for the two years (Fig. 7): the higher the $Ca^{2+}$ concentration, the higher the inter-annual carbonate growth rate.

*Degassing process.* – The precipitation of carbonate in a cave is driven by the degassing of $CO_2$ from drip water, which increases the SI value of the solution (Holland *et al.* 1964; De Choudens-Sanchez & Gonzalez 2009). The degassing process is controlled mainly by the cave-air $CO_2$ concentration. A low cave-air $CO_2$ concentration will drive $CO_2$ degassing from drip water quickly, which in turn will yield high SI values of the drips and increase the precipitation rate. Conversely, a

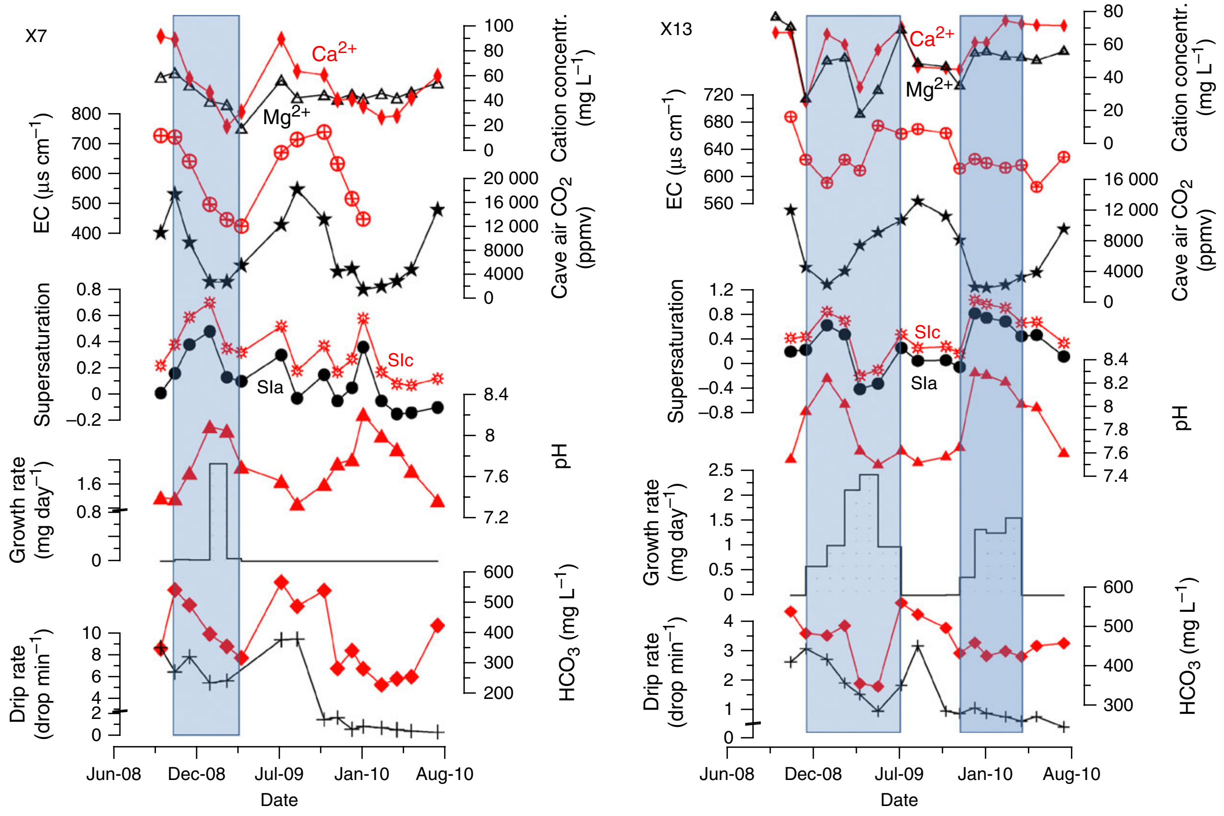

*Fig. 7.* Variations in hydrochemical parameters, drip rate and growth rate for the period between August 2008 and August 2010. X7 and X13 indicate drip sites. The blue bars indicate the periods when modern carbonates precipitated. This figure is available in colour at http://www.boreas.dk.

high cave-air $CO_2$ concentration may inhibit degassing and reduce the carbonate precipitation rate (Baker *et al.* 1998; Banner *et al.* 2007). In Xianren Cave, the cave-air $CO_2$ concentration is lowest in winter, so the precipitation rate is highest then. In summer, the highest cave-air $CO_2$ concentration coincides with the lowest precipitation rate (near zero) (Fig. 7). The result agrees well with the previous study in Shihua Cave, China (Cai *et al.* 2011).

In Xianren Cave, the seasonal variation of cave-air $CO_2$ concentration follows the patterns of atmospheric temperature and rainfall (Fig. 6). A number of studies have shown the same pattern as in Xianren Cave and analysed the possible mechanisms as follows. During summer, relatively warm outside air and relatively stable high-pressure weather systems lead to stagnant cave air with high $CO_2$ concentration. During winter, caves are often well ventilated as a consequence of relatively cold and dense outside air (with low atmospheric $CO_2$ levels) displacing warmer, higher-$CO_2$ cave air (Buecher 1999; Spötl *et al.* 2005; Banner *et al.* 2007).

Moreover, the degassing process may be further affected by the drip rate, which is directly related to the duration of time over which degassing takes place (Dreybrodt 1988). If the drip rate is too high, the duration of time over two drips will be too short to make the $CO_2$ degas completely from the water film on the top of the stalagmite. In Xianren Cave during the rainy season, the highest drip rate causes a near-zero precipitation rate. At the other extreme, if the drip time is significantly longer than that required for complete degassing, the growth rate will become slow as there is not sufficient water to replace each drip (Genty *et al.* 2001). Thus, during late spring in Xianren Cave the drip rates are too slow to cause carbonate precipitation (Fig. 7). When the drip rate is moderate, not only allowing complete degassing but also providing enough discharge to the stalagmite top, the precipitation rate will be highest. For instance, the highest precipitation rate in Xianren Cave occurs during the winter, when the drip rates are moderate (Fig. 7).

In summary, the factors that directly control the intra-annual growth rate of a stalagmite are the pH value and the drip rate, which in turn are controlled mainly by cave-air $CO_2$ concentration and local rainfall, respectively. The main factor that controls the inter-annual growth rate is $Ca^{2+}$ concentration, which in turn may be controlled by local atmospheric temperature and rainfall. During the two years, the variation in temperature was very small, while that of rainfall was very large (Fig. 7). This implies that the modern annual carbonate precipitation rate may be controlled mainly by rainfall.

### *The growth process of the annual laminae made up of compact and porous aragonitic sub-layers*

By comparing the mineral composition and crystal structures of stalagmite laminae with modern carbonates precipitating on glass slides in Xianren Cave, we can infer the conditions under which the compact and porous sub-layers form. The compact sub-layer is composed of elongated columnar aragonite crystals (Fig. 1B) (Duan *et al.* 2010), which are similar to the crystals of modern carbonate precipitated on glass slides: during the second hydrologic year, when it started to precipitate in winter, elongated columnar aragonite with few crystal defects formed first (Fig. 1D). The environment under which the elongated columnar aragonite formed is such that the drip rate is moderate, which results in prolonged degassing (Fig. 8), as reported previously (Frisia *et al.* 2002). That is because there is enough time and discharge for aragonite to crystallize following its crystal habit. As a result, the crystal structure is perfect.

The elongated columnar aragonites grow in one direction along their c-axes so that the intercrystalline spaces are few and form the compact sub-layer (Fig. 1B, D).

The porous sub-layer is made up of needle aragonites forming radiating masses (Fig. 1C), and we observed the same crystals in modern carbonates in the spring of 2010 from late January to March (Fig. 1E). The conditions under which they formed are characterized by a higher Mg/Ca ratio and lower discharge, as reported previously (Frisia *et al.* 2002). Samples with higher crystal defect density and more irregular morphology along the growth surface reflect periods when drip rates are at their lowest or cease completely (Frisia *et al.* 2000; Treble *et al.* 2005). When the time lapse between two drops splashing at the top of a stalagmite is long, the drip water cannot discharge in time. Therefore, the water film formed on the top of the stalagmite will become thinner and thinner while it diffuses from centre to brim, resulting in $CO_2$ degassing quickly, so that the water film will be under instantaneous supersaturation. In turn, needle aragonite will crystallize quickly from the water film, with rough faces and defects and more varied orientations, forming radiating masses (Fig. 1E). Furthermore, when SIa is low, the presence of growth inhibitors, such as $Mg^{2+}$, may cause the formation of highly defective crystallites with poorly ordered stacking (Frisia *et al.* 2000).

### *The climatic signal indicated by the occurrence of primary calcites in aragonitic stalagmite*

Aragonitic speleothems are usually found in caves in dolomite, for example in South Africa (Holmgren *et al.* 1994), France, the USA, Israel (Railsback *et al.* 1994) and Brazil (Bertaux *et al.* 2002). However, calcite speleothems are usually formed in caves in limestone. An example is Panlong Cave: although it is only about 3 km away from Xianren Cave, all the speleothems there are composed of calcites. This suggests that the essential factor that controls the mineral composition of stalagmites is not the climate but the surrounding lithology.

In Xianren Cave, although the stalagmite is composed mainly of aragonite laminae, some exceptional parts of the stalagmite laminae (Fig. 2A, B) show a visible alternation of bulk calcites (Fig. 2C) and needle aragonites (Fig. 2D). Interestingly, we found both polymorphs of carbonate in modern carbonate deposits in Xianren Cave. When it started to precipitate during the winter of 2008, rhombohedral calcites (Fig. 2E) formed first on the glass slides at all study sites. In the spring, needle aragonites (Fig. 2F) gradually formed at all sites. Therefore, some processes other than the surrounding lithology (such as climate change) may also affect the paramorphs of carbonate.

As suggested by abundant experimental and empirical work, when the SI is low, increasing Mg/Ca will decrease the growth rate of calcite while the aragonite growth rate is unaffected (Kitano 1962; Fyfe & Bischoff 1965; Pytkowicz 1965; Bischoff & Fyfe 1968; Berner 1975; Morse 1983; Burton & Walter 1987; Fairchild *et al.* 1996; Fernandez-Diaz *et al.* 1996; Davis *et al.* 2000). In turn, the Mg/Ca of drip water is affected by drip rate (Fairchild *et al.* 1996; Frisia *et al.* 1997). A low drip rate tends to promote longer mean residence times of percolating water, leading to more prior calcite precipitation, which results in an increased Mg/Ca of drip water (Fairchild *et al.* 2000; Genty *et al.* 2001; Spötl *et al.* 2005). Our results are consistent with earlier studies. When calcite formed, the geochemical parameters of the drip water were moderate drip rate, high SI and $Mg/Ca < 1.5$ (Fig. 8). When needle aragonites formed, both the drip rate and SI value were lower than those for calcite formation, and $Mg/Ca > 1.5$ (Fig. 8).

The main differences between the weather conditions of the two years are as follows. In the first hydrologic year, the rainfall was much higher than the local average annual precipitation from 1954 to 2010 (Fig. 5), resulting in a higher drip rate and lower Mg/Ca (Fig. 7), whereas in the second hydrologic year, the rainfall was less, resulting in a lower drip rate (Fig. 4) and higher Mg/Ca (Fig. 8). In accordance with the weather conditions, the mineral composition of modern carbonates showed inter-annual variations in the two years. Calcites formed only in the first hydrologic year (Fig. 8). Hence, the crystallographic features may be linked to climate changes.

In monsoonal climates, calcite crystallization is favoured in many stalagmites during the wet season, whereas aragonite is favoured during the relatively dry inter-monsoon months (Railsback *et al.* 1994; Frisia

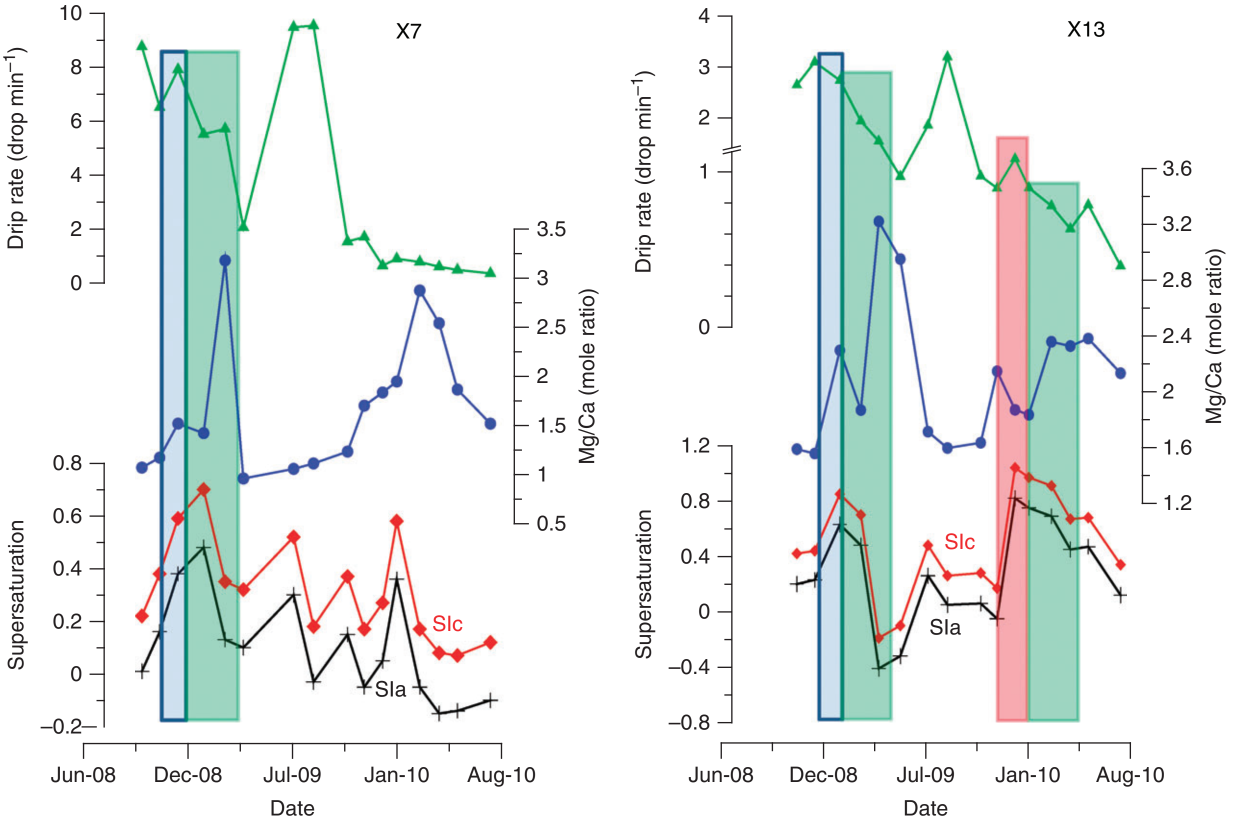

*Fig. 8.* The main factors controlling the mineral composition and crystal structures of modern stalagmites. X7 and X13 indicate drip sites. Periods when calcite, elongated columnar aragonite and needle aragonite were formed are shown by the blue bar, red bar and green bar, respectively. This figure is available in colour at http://www.boreas.dk.

*et al.* 1997). A decrease in the intensity of precipitation during the monsoon period could therefore result in aragonite precipitation throughout the entire year (Dennisston *et al.* 2000). In other words, we can infer that the presence of calcite in aragonitic stalagmite could be used as an indicator of palaeo-wetness, which agrees with the previous study of Railsback *et al.* (1994).

### *Implications for palaeoclimate reconstruction*

The variable crystal structures of sub-layers, which are controlled by the seasonal variations in climate, may be used as a seasonal-resolution proxy of climate. For instance, stalagmite laminae described by Genty & Quinif (1996) consist of a white-porous calcite sub-layer and a dark compact calcite sub-layer. The authors interpreted the annual laminae as a proxy reflecting seasonal variation of water excess. In this study, we have examined the growth process of aragonitic stalagmite laminae in Xianren Cave, which may be of use in high-resolution climate reconstructions in future work. Furthermore, we also found some calcite in the aragonitic stalagmite, which may reflect an increase in the intensity of precipitation during the rainy season in that year.

## Conclusion

Based on the mineralogy and crystal growth of stalagmite laminae and the cave monitoring data, we draw the following conclusions.

- Almost all the carbonate precipitation occurs in winter and spring (dry seasons), when the cave-air $CO_2$ concentration is low and the drip rate is moderate.
- The stalagmite laminae of Xianren Cave are annual layers consisting of a compact sub-layer composed of elongated columnar aragonites with a general longitudinal orientation (parallel to the vertical growth axis) and a porous sub-layer that is composed mainly of needle aragonites forming radiating masses.
- The compact sub-layer forms in winter when the drip rate is moderate and the degassing is slow, continuous and prolonged. The porous sub-layer forms in early spring when the drip rate is slow and Mg/Ca is higher.
- The exceptional occurrence of calcite in aragonitic stalagmite could be an indicator of rainy and moist weather conditions.

*Acknowledgements.* – We are grateful to Professor Andy Baker for his constructive comments. We thank the administrative committee of Xianren Cave for field assistance. We especially thank the reviewer

Professor Ian J. Fairchild for his constructive comments and the software he sent to us to check and interpret the results. We thank another anonymous reviewer and the Editor-in-Chief, Professor Jan A. Piotrowski, for their constructive suggestions and help with the English. We also thank Dr Taijin Lu for his help with the English. This work was supported by the National Basic Research Program of China (Grant No. 2010CB950201) and the National Natural Science Foundation of China (Grant Nos 40772213 and 41030103) and Special Foundation Work (Grant No. 2011FY120300).

## References

Baker, A. & Genty, D. 1998: Environmental pressures on conserving cave speleothems: effects of changing surface land use and increased cave tourism. *Journal of Environmental Management 53*, 165–175.

Baker, A., Genty, D., Dreybrodt, W., Barnes, W. L., Mockler, N. J. & Grapes, J. 1998: Testing theoretically predicted stalagmite growth rate with Recent annually laminated samples: Implications for past stalagmite deposition. *Geochimica et Cosmochimica Acta 62*, 393–404.

Baker, A., Smart, P. L., Edwards, R. L. & Richards, D. A. 1993: Annual growth banding in a cave stalagmite. *Nature 364*, 518–520.

Ban, F., Pan, G., Zhu, J., Cai, B. & Tan, M. 2008: Temporal and spatial variations in the discharge and dissolved organic carbon of drip waters in Beijing Shihua Cave, China. *Hydrological Processes 22*, 3749–3758.

Banner, J. L., Guilfoyle, A., James, E. W., Stern, L. A. & Musgrove, M. 2007: Seasonal variations in modern speleothem calcite growth in Central Texas, USA. *Journal of Sedimentary Research 77*, 615–622.

Bar-Matthews, M., Matthews, A. & Ayalon, A. 1991: Environmental controls of speleothem mineralogy in a karstic dolomitic terrain (Soreq Cave, Israel). *The Journal of Geology 99*, 189–207.

Berner, R. 1975: The role of magnesium in the crystal growth of calcite and aragonite from sea water. *Geochimica et Cosmochimica Acta 39*, 489–494.

Bertaux, J., Sondag, F., Santos, R., Soubies, F., Causse, C., Plagnes, V., Le Cornec, F. & Seidel, A. 2002: Paleoclimatic record of speleothems in a tropical region: study of laminated sequences from a Holocene stalagmite in Central-West Brazil. *Quaternary International 89*, 3–16.

Bischoff, J. & Fyfe, W. 1968: Catalysis, inhibition, and the calcite–aragonite problem; Part 1, The aragonite–calcite transformation. *American Journal of Science 266*, 65–79.

Brook, G. A., Sheen, S.-W., Rafter, M. A., Railsback, L. B. & Lundberg, J. 1999: A high-resolution proxy record of rainfall and ENSO since AD 1550 from layering in stalagmites from Anjohibe Cave, Madagascar. *The Holocene 9*, 695–705.

Buecher, R. 1999: Microclimate study of Kartchner caverns, Arizona. *Journal of Cave and Karst Studies 61*, 108–120.

Burton, E. & Walter, L. 1987: Relative precipitation rates of aragonite and Mg calcite from seawater: Temperature or carbonate ion control? *Geology 15*, 111–114.

Cai, B., Pumijumnong, N., Tan, M., Muangsong, C., Kong, X., Jiang, X. & Nan, S. 2010: Effects of intraseasonal variation of summer monsoon rainfall on stable isotope and growth rate of a stalagmite from northwestern Thailand. *Journal of Geophysical Research 115*, D21104, doi:10.1029/2009JD013378.

Cai, B., Zhu, J., Ban, F. & Tan, M. 2011: Intra-annual variation of the calcite deposition rate of drip water in Shihua Cave, Beijing, China and its implications for palaeoclimatic reconstructions. *Boreas*, *40*, 525–535.

Davis, K., Dove, P. & De Yoreo, J. 2000: The role of $Mg^{2+}$ as an impurity in calcite growth. *Science 290*, 1134–1137.

De Choudens-Sanchez, V. & Gonzalez, L. A. 2009: Calcite and aragonite precipitation under controlled instantaneous supersaturation: elucidating the role of $CaCO_3$ saturation state and Mg/Ca ratio on calcium carbonate polymorphism. *Journal of Sedimentary Research 79*, 363–376.

Denniston, R. F., Gonzalez, L. A., Asmerom, Y., Sharma, R. H. & Reagan, M. K. 2000: Speleothem evidence for changes in Indian summer monsoon precipitation over the last ~2300 years. *Quaternary Research 53*, 196–202.

Dreybrodt, W. 1988: *Processes in Karst Systems – Physics, Chemistry and Geology*. 287 pp. Springer, Berlin.

Dreybrodt, W. 1999: Chemical kinetics, speleothem growth and climate. *Boreas 28*, 347–356.

Duan, W., Tan, M., Cheng, H. & Zhang, Y. 2010: Intra-annual structure of aragonitic stalagmite laminae from Yunnan Xianren Cave: SEM. *Quaternary Sciences 30*, 1066–1067.

Fairchild, I., Tooth, A., Huang, Y., Borsato, A., Frisia, S. & McDermott, F. 1996: Spatial and temporal variations in water and stalactite chemistry in currently active caves: a precursor to interpretations of past climate. *In* Bottrell, S. H. (ed.): *Proceedings of the Fourth International Symposium on the Geochemistry of the Earth's Surface*, 229–233. University of Leeds, Ilkley.

Fairchild, I. J., Borsato, A., Tooth, A. F., Frisia, S., Hawkesworth, C. J., Huang, Y., McDermott, F. & Spiro, B. 2000: Controls on trace element (Sr-Mg) compositions of carbonate cave waters: implications for speleothem climatic records. *Chemical Geology 166*, 255–269.

Fairchild, I. J., Frisia, S., Borsato, A. & Tooth, A. F. 2007: Speleothems. *In* Nash, D. J. & McLaren, S. J. (eds): *Geochemical Sediments and Landscapes*, 200–245. Blackwell, Oxford.

Fernandez-Diaz, L., Putnis, A., Prieto, M. & Putnis, C. 1996: The role of magnesium in the crystallization of calcite and aragonite in a porous medium. *Journal of Sedimentary Research 66*, 482–491.

Frisia, S., Borsato, A., Fairchild, I. J. & Longinelli, A. 1997: Aragonite precipitation at Grotte de Clamouse (Herault, France): role of magnesium and drip rate. *In* Jeannin, P.-Y. (ed.): *Physical Speleology and Karst Geomorphology: 12th International Congress of Speleology*, 247–250. La Chaux-de-Fonds.

Frisia, S., Borsato, A., Fairchild, I. J. & McDermott, F. 2000: Calcite fabrics, growth mechanisms, and environments of formation in speleothems from the Italian Alps and southwestern Ireland. *Journal of Sedimentary Research 70*, 1183–1196.

Frisia, S., Borsato, A., Fairchild, I. J., McDermott, F. & Selmo, E. M. 2002: Aragonite-calcite relationships in speleothems (Grotte de Clamouse, France): Environment, fabrics, and carbonate geochemistry. *Journal of Sedimentary Research 72*, 687–699.

Frisia, S., Borsato, A., Preto, N. & McDermott, F. 2003: Late Holocene annual growth in three Alpine stalagmites records the influence of solar activity and the North Atlantic Oscillation on winter climate. *Earth and Planetary Science Letters 216*, 411–424.

Fyfe, W. S. & Bischoff, J. L. 1965: The calcite–aragonite problem. *In* Pray, L. C. & Murray, R. C. (eds): *Dolomitization and Limestone Diagenesis: A Symposium. Society for Sedimentary Geology*, *Special Publication*, *13*, 3–13.

Genty, D. 1992: Les spéléothèmes du tunnel de Godarville (Belgique) - un exemple exceptionnel de concrétionnement moderne - intérêt pour l'étude de la cinétique de la précipitation de la calcite et de sa relation avec les variations d'environnement. *Speleochronos 4*, 3–29.

Genty, D. & Quinif, Y. 1996: Annually laminated sequences in the internal structure of some Belgian stalagmites – Importance for paleoclimatology. *Journal of Sedimentary Research 66*, 275–288.

Genty, D., Baker, A. & Vokal, B. 2001: Intra- and inter-annual growth rate of modern stalagmites. *Chemical Geology 176*, 191–212.

Holland, H. D., Kirsipu, T. V., Huebner, J. S. & Oxburgh, U. M. 1964: On some aspects of the chemical evolution of cave waters. *The Journal of Geology 72*, 36–67.

Holmgren, K., Lauritzen, S.-E. & Possnert, G. 1994: $^{230}Th^{234}U$ and $^{14}C$ dating of a late Pleistocene stalagmite in Lobatse II Cave, Botswana. *Quaternary Science Reviews 13*, 111–119.

Kitano, Y. 1962: The behavior of various inorganic ions in the separation of calcium carbonate from a bicarbonate solution. *Bulletin of the Chemical Society of Japan 35*, 1973–1980.

Mattey, D., Lowry, D., Duffet, J., Fisher, R., Hodge, E. & Frisia, S. 2008: A 53 year seasonally resolved oxygen and carbon isotope record from a modern Gibraltar speleothem: Reconstructed drip water and relationship to local precipitation. *Earth and Planetary Science Letters 269*, 80–95.

Morse, J. 1983: The kinetics of calcium carbonate dissolution and precipitation. *Reviews in Mineralogy and Geochemistry 11*, 227–264.

Polyak, V. J. & Asmerom, Y. 2001: Late Holocene climate and cultural changes in the southwestern United States. *Science 294*, 148–151.

Proctor, C. J., Baker, A., Barnes, W. L. & Gilmour, M. A. 2000: A thousand year speleothem proxy record of North Atlantic climate from Scotland. *Climate Dynamics 16*, 815–820.

Pytkowicz, R. 1965: Rates of inorganic calcium carbonate nucleation. *The Journal of Geology 73*, 196–199.

Railsback, L. B., Brook, G. A., Chen, J., Kalin, R. & Fleisher, C. J. 1994: Environmental controls on the petrology of a late Holocene speleothem from Botswana with annual layers of aragonite and calcite. *Journal of Sedimentary Research 64*, 147–155.

Rossum, J. R. 1975: Checking the accuracy of water analyses through the use of conductivity. *Journal of American Water Works Association 67*, 204–205.

Ruan, J. & Hu, C. 2010: Seasonal variations and environmental controls on stalagmite calcite crystal growth in Heshang Cave, central China. *Chinese Science Bulletin 55*, 3929–3935.

Self, C. & Hill, C. 2003: How speleothems grow: an introduction to the ontogeny of cave minerals. *Journal of Cave and Karst Studies 65*, 130–151.

Soubies, F., Seidel, A., Mangin, A., Genty, D., Ronchail, J., Plagnes, V., Hirooka, S. & Santos, R. 2005: A fifty-year climatic signal in three Holocene stalagmite records from Mato Grosso, Brazil. *Quaternary International 135*, 115–129.

Spötl, C., Fairchild, I. J. & Tooth, A. F. 2005: Cave air control on dripwater geochemistry, Obir Caves (Austria): Implications for speleothem deposition in dynamically ventilated caves. *Geochimica et Cosmochimica Acta 69*, 2451–2468.

Tan, M. & Liu, T. 2003: Cyclic rapid warming on centennial-scale revealed by a 2650-year stalagmite record of warm season temperature. *Geophysical Research Letters 30*, 1617–1620.

Tan, M., Liu, T., Qin, X. & Zhang, D. 1997: Microbanding of stalagmite and its significance. *PAGES News 5*, 6–7.

Tan, M., Pan, G., Wang, X., Qin, X., Teng, Y., Song, L. & Lin, Y. 1999: Stalagmite and environment preliminary study on the formation of laminated stalagmites. *Carsologica Sinica 18*, 197–205.

Treble, P. C., Chappell, J. & Shelley, J. M. G. 2005: Complex speleothem growth processes revealed by trace element mapping and scanning electron microscopy of annual layers. *Geochimica et Cosmochimica Acta 69*, 4855–4863.

Yadava, M. G., Ramesh, R. & Pant, G. B. 2004: Past monsoon rainfall variations in peninsular India recorded in a 331-year-old speleothem. *The Holocene 14*, 517–524.